

1-31-2011

## $\beta$ -decay studies of the transitional nucleus Cu75 and the structure of Zn75

S. V. Ilyushkin  
*Mississippi State University*

J. A. Winger  
*Mississippi State University*

K. P. Rykaczewski  
*ORNL Physics Division*

C. J. Gross  
*ORNL Physics Division*

J. C. Batchelder  
*Oak Ridge Associated Universities*

*See next page for additional authors*

Follow this and additional works at: [https://repository.lsu.edu/physics\\_astronomy\\_pubs](https://repository.lsu.edu/physics_astronomy_pubs)

---

### Recommended Citation

Ilyushkin, S., Winger, J., Rykaczewski, K., Gross, C., Batchelder, J., Cartegni, L., Darby, I., Grzywacz, R., Hamilton, J., Korgul, A., Królas, W., Liddick, S., Mazzocchi, C., Mendez, T., Padgett, S., Rajabali, M., Shapira, D., Stracener, D., & Zganjar, E. (2011).  $\beta$ -decay studies of the transitional nucleus Cu75 and the structure of Zn75. *Physical Review C - Nuclear Physics*, 83 (1) <https://doi.org/10.1103/PhysRevC.83.014322>

This Article is brought to you for free and open access by the Department of Physics & Astronomy at LSU Scholarly Repository. It has been accepted for inclusion in Faculty Publications by an authorized administrator of LSU Scholarly Repository. For more information, please contact [ir@lsu.edu](mailto:ir@lsu.edu).

---

**Authors**

S. V. Ilyushkin, J. A. Winger, K. P. Rykaczewski, C. J. Gross, J. C. Batchelder, L. Cartegni, I. G. Darby, R. Grzywacz, J. H. Hamilton, A. Korgul, W. Królas, S. N. Liddick, C. Mazzocchi, T. Mendez, S. Padgett, M. M. Rajabali, D. Shapira, D. W. Stracener, and E. F. Zganjar



# CHORUS

This is the accepted manuscript made available via CHORUS. The article has been published as:

## $\beta$ -decay studies of the transitional nucleus $^{75}\text{Cu}$ and the structure of $^{75}\text{Zn}$

S. V. Ilyushkin, J. A. Winger, K. P. Rykaczewski, C. J. Gross, J. C. Batchelder, L. Cartegni, I. G. Darby, R. Grzywacz, J. H. Hamilton, A. Korgul, W. Królas, S. N. Liddick, C. Mazzocchi, T. Mendez, S. Padgett, M. M. Rajabali, D. Shapira, D. W. Stracener, and E. F. Zganjar

Phys. Rev. C **83**, 014322 — Published 31 January 2011

DOI: [10.1103/PhysRevC.83.014322](https://doi.org/10.1103/PhysRevC.83.014322)

The  $\beta$  decay studies of the transitional nucleus  $^{75}\text{Cu}$  and the structure of  $^{75}\text{Zn}$  \*

S. V. Ilyushkin,<sup>1,†</sup> J. A. Winger,<sup>1</sup> K. P. Rykaczewski,<sup>2</sup> C. J. Gross,<sup>2</sup> J. C. Batchelder,<sup>3</sup> L. Cartegni,<sup>4</sup> I. G. Darby,<sup>4,5</sup> R. Grzywacz,<sup>2,4</sup> J. H. Hamilton,<sup>6</sup> A. Korgul,<sup>4,6,7,8</sup> W. Królas,<sup>8,9</sup> S. N. Liddick,<sup>4,10</sup> C. Mazzocchi,<sup>4,7,11</sup> T. Mendez,<sup>2</sup> S. Padgett,<sup>4</sup> M. M. Rajabali,<sup>4,5</sup> D. Shapira,<sup>2</sup> D. W. Stracener,<sup>2</sup> and E. F. Zganjar<sup>12</sup>

<sup>1</sup>Department of Physics and Astronomy, Mississippi State University, Mississippi State, Mississippi 39762, USA

<sup>2</sup>Physics Division, Oak Ridge National Laboratory, Oak Ridge, Tennessee 37831, USA

<sup>3</sup>UNIRIB, Oak Ridge Associated Universities, Oak Ridge, Tennessee 37831, USA

<sup>4</sup>Department of Physics and Astronomy, University of Tennessee, Knoxville, Tennessee 37996, USA

<sup>5</sup>Instituut voor Kern-en Stralingsfysica, Katholieke Universiteit Leuven, Leuven B-3001, Belgium

<sup>6</sup>Department of Physics and Astronomy, Vanderbilt University, Nashville, Tennessee 37235, USA

<sup>7</sup>Faculty of Physics, University of Warsaw, Warszawa PL 00-681, Poland

<sup>8</sup>Joint Institute for Heavy-Ion Reactions, Oak Ridge, Tennessee 37831 USA

<sup>9</sup>Institute of Nuclear Physics, Polish Academy of Sciences, Kraków PL 31-342, Poland

<sup>10</sup>National Superconducting Cyclotron Laboratory,

Michigan State University, East Lansing, Michigan 48824, USA

<sup>11</sup>Università degli Studi di Milano and INFN, Sez. Milano, Milano I-20133, Italy

<sup>12</sup>Department of Physics and Astronomy, Louisiana State University, Baton Rouge, Louisiana 70803, USA

The  $\beta$  decay of  $^{75}\text{Cu}$  ( $t_{1/2} = 1.222(8)\text{s}$ ) to levels in  $^{75}\text{Zn}$  has been studied at the Holifield Radioactive Ion Beam Facility of Oak Ridge National Laboratory. The  $\gamma\gamma$  and  $\beta\gamma$  data were collected at the Low-energy Radioactive Ion Beam Spectroscopy Station using the high-resolution isobar separator to obtain a purified  $^{75}\text{Cu}$  beam with a rate of over 2000 ions per second. The excited states in  $^{75}\text{Zn}$  have been identified for the first time. A total of 120  $\gamma$ -ray transitions were placed in a level scheme containing 59 levels including two states above the neutron separation energy and a previously unknown  $1/2^-$  isomeric state at 127 keV. Spins and parities of several states were deduced and interpreted based on the observed  $\beta$  feeding and  $\gamma$  decay pattern.

PACS numbers: 23.20.Lv, 23.35.+g, 27.50.+e, 29.38.-c

## I. INTRODUCTION

Acquiring empirical information on nuclei with large neutron-to-proton asymmetry, with respect to the stable isotopes, leads us to better understanding of the nucleon-nucleon interactions in nuclear matter. In particular, the evolution of single particle properties can now be studied for very neutron-rich systems, where the sequence of orbitals known near the  $\beta$ -stability path has been proven inadequate in describing properties of exotic isotopes [1–3].

Having just one particle outside the closed  $Z=28$  core makes copper a logical choice to study the strength of the shell effects and particularly the details of the residual interactions. In a traditional shell model view, a single-particle coupling suggests  $J^\pi = 3/2^-$  for the ground-state spin and parity in odd-A copper owing to the 29<sup>th</sup> proton being in the  $\pi 2p_{3/2}$  single particle orbital. Earlier works [4, 5] confirmed this prediction by observing  $\beta$ -feeding to

the  $J^\pi = 1/2^-$  and  $5/2^-$  states in the zinc daughter nuclei for the odd-A copper isotopes up to  $^{73}\text{Cu}$ . However, energy level systematics for  $^{69-73}\text{Cu}$  (Fig. 1) indicate a lowering of the  $5/2^-$  state relative to the  $3/2^-$  ground state. Recently, a combination of in-source and collinear laser spectroscopy measurements of the hyperfine structure of  $^{75}\text{Cu}$  revealed  $\mu(^{75}\text{Cu}) = +1.0062(13)\mu_N$  corresponding to spin  $J = 5/2$  for  $^{75}\text{Cu}$  [6]. Additionally, both recently completed studies on  $\beta$  decay of  $^{77}\text{Cu}$  [7, 8] suggest  $5/2^-$  for its ground state. This behavior is consistent with theoretical calculations in this region [9] predicting changes in the  $\pi 2p_{3/2} - \pi 1f_{5/2}$  orbital ordering due to the monopole component of the residual nucleon-nucleon interaction. The  $\beta$  decay properties of

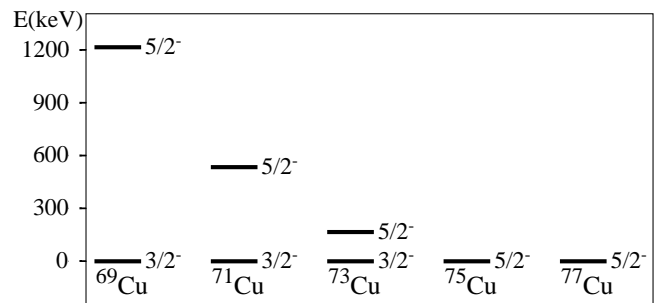


FIG. 1: Low-energy level systematics of odd-A copper isotopes. (See text for references.)

\*Notice: This manuscript has been authored by UT-Battelle, LLC, under Contract No. DE-AC05-00OR22725 with the U.S. Department of Energy. The United States Government retains and the publisher, by accepting the article for publication, acknowledges that the United States Government retains a non-exclusive, paid-up irrevocable, world-wide license to publish or reproduce the published form of the manuscript, or allow others to do so, for United States Government purposes.

†Electronic address: svi1@msstate.edu

$^{75}\text{Cu}$  are of current concern as this nuclide lies near the  $\pi 2p_{3/2} - \pi 1f_{5/2}$  orbital crossing point, while  $\beta$  decay information is very limited. Prior to this study, the only data available on the  $\beta$  decay of  $^{75}\text{Cu}$  included its half-life (1.224(3)s [10]) and delayed-neutron emission probability ( $3.5 \pm 0.6\%$  [11]). Information concerning the low-lying levels of the odd- $A$  zinc ( $Z = 30$ ) isotopes with  $A = 67, 69, 71$  is known from  $\beta$ -decay and ( $d, p$ ) neutron transfer reaction studies [12, 13]. The structure of  $^{73}\text{Zn}$  was investigated with a multi-nucleon transfer reaction [14] as well as the  $\beta$  decay of  $^{73}\text{Cu}$  produced in the fragmentation of a  $^{76}\text{Ge}$  beam in a beryllium target [5]. Finally, states in  $^{77}\text{Zn}$  are known from  $\beta$ -decay studies [7, 8]. However, no information on excited states in  $^{75}\text{Zn}$  has been available.

Of special interest for the odd- $A$  zinc isotopes is the evolution of the  $1/2^-$  state relative to the  $9/2^+$  and  $7/2^+$  states. The  $9/2^+$  state is observed (Fig. 2, lower panel) to progressively decrease in energy relative to the  $1/2^-$  state with each additional neutron pair to the  $1g_{9/2}$  orbital up to  $N = 41$ , where this state could be expected to become the ground state with one  $\nu 1g_{9/2}$  particle above the  $N=40$  core. The observation that the ground state of  $^{71}\text{Zn}$  is  $1/2^-$  may be due to the stronger pair binding in the  $\nu 1g_{9/2}$  orbital. The  $9/2^+$  state has not been identified in  $^{73}\text{Zn}$ , however a possible  $7/2^+$  state which would be associated with the  $\nu 1g_{9/2}$  orbital has been reported. However, there exists some controversy about this state as discussed in the following paragraph. Both the  $7/2^+$  ground state and  $9/2^+$  first excited state have been tentatively assigned in  $^{77}\text{Zn}$  where the  $9/2^+$  state lies  $\sim 600$  keV below the  $1/2^-$  state [7]. Identifying the  $1/2^-$  and  $9/2^+$  states in  $^{75}\text{Zn}$  shall complete the information on the evolution of shell structure near Fermi level

in this region.

A comparison of the systematics of the zinc and germanium energy levels illustrates the similarities in the overall low-energy structure between these two isotopic chains up to  $N = 43$  as seen in Fig. 2. One exception is  $^{73}\text{Zn}$  where a comparison with its isotonic counterpart ( $^{75}\text{Ge}$ ) suggests the existence of three low-lying positive parity states, though only one state has been clearly observed in  $\beta$  decay studies [5, 14]. A 5.8 s half-life for a state depopulated by 42.1- and 195.5-keV  $\gamma$  rays was reported in the  $\beta$ -decay studies of the  $A = 73$  group for even- $Z$  nuclei [14]. The 195.5-keV transition was deduced to have  $E3$  multipolarity and assigned to the isomeric decay of  $^{73}\text{Zn}$ , while the 42-keV transition was assumed to be from a state in  $^{73}\text{Ga}$ . However, in a subsequent  $\beta$ -decay study [5], a 195.5-keV  $\gamma$  ray was observed whose transition probability was found to be greater with a half-life measured as 13.0 ms which implies a larger  $M2$  admixture. These two apparently contradictory observations could be accounted for by the presence of two closely spaced levels in  $^{73}\text{Zn}$  with the 5.8 s 195.5-keV isomer observed earlier [14] likely to be the  $7/2^+$  level expected at low energy according to the level systematics. In addition, the  $E3$  character of the isomeric transitions in most neighboring nuclei has been established by internal conversion measurements (see, for example, Ref. [16] and references therein). Further, the occurrence of a triplet of positive parity states having  $J^\pi = 5/2^+, 7/2^+$ , and  $9/2^+$  has also been predicted by particle-triaxial rotor model calculations assuming a ground state quadrupole deformation of  $\beta_2 = 0.20$  [5]. Although, the predicted  $9/2^+$  state seems a particularly tempting candidate for placement of the 42-keV  $\gamma$  ray, its location was substantiated by the half-life analysis of copper and gallium K X-rays and the fact that the 42-keV transition was seen in  $\beta\gamma$  coincidence spectra [14] to be a transition in  $^{73}\text{Ga}$ . The NSCL experiment [5] was not conclusive on this point since 42 keV was below their energy threshold thus leaving existence of a  $7/2^+$  state in  $^{73}\text{Zn}$  uncertain. It therefore appears that  $^{73}\text{Zn}$  and  $^{75}\text{Ge}$  do have very similar structures. The question then becomes why the level structure in  $^{77}\text{Zn}$  differs so radically from that of its neighboring  $N = 47$  isotope  $^{79}\text{Ge}$  and will a similar change be observed for  $^{75}\text{Zn}$ .

Another peculiarity related to the structure of  $^{75}\text{Zn}$  is isomerism. Although, isomerism is certainly expected in  $^{75}\text{Zn}$  due to the proximity of  $\nu 2p_{1/2}$  and  $\nu 1g_{9/2}$  orbitals, it has not been observed. Again, analysis of neighboring nuclei (Fig. 3) shows that all even- $Z$ ,  $N=45$  isotones are observed to have a three-quasi-particle type  $7/2^+$  ground state, a consequence of Coriolis mixing of three neutrons in the  $1g_{9/2}$  orbital [17] and a  $1/2^-$  isomeric state due to the nearby  $\nu 2p_{1/2}$  orbital. It has been suggested [18] that the  $1/2^-$  state in  $^{75}\text{Zn}$  might have a very short half-life caused by the presence of a  $5/2^+$  intruder state located below it or a half-life comparable to that of the ground state such that the  $\gamma$ -rays are thus not easily assigned to a specific isomer. The latter hypothesis was rejected on the

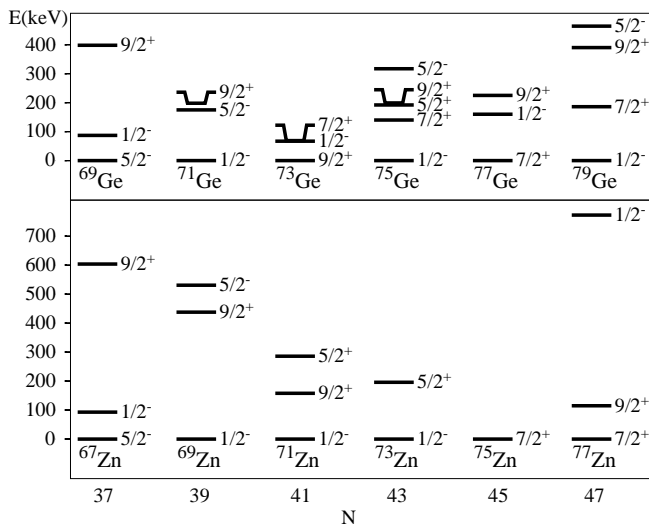


FIG. 2: Low-energy level systematics of odd- $A$   $Z=30$  zinc (lower panel) and  $Z=32$  germanium (upper panel) isotopes. Levels in germanium are taken from [15], those in zinc from [5], [12], and [13]. For discussion, see text.

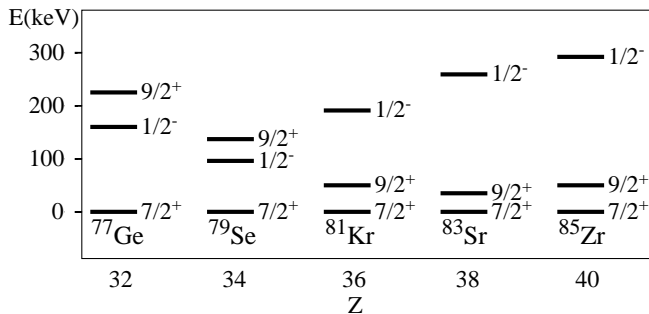


FIG. 3: Low-energy level systematics of odd-A  $N = 45$  isotones. Levels are taken from [15]. For discussion, see text.

basis of available data on the  $\beta$  decay of  $^{75}\text{Zn}$ , although this is insufficient evidence to assert the non-existence of isomerism.

It is apparent that  $^{75}\text{Zn}$  lies at a transition point in nuclear structure. Therefore, determination of the energies of the  $1/2^-$  and  $9/2^+$  states could provide a better understanding of the evolution of structure in this region. This work extends our knowledge on the  $\beta$  decay properties of  $^{75}\text{Cu}$  presenting the first detailed level structure of  $^{75}\text{Zn}$ . Evidence will also be presented for a low-lying  $\beta$ -decaying isomeric state.

## II. EXPERIMENTAL TECHNIQUE

The experiment was performed at the Holifield Radioactive Ion Beam Facility [19] of Oak Ridge National Laboratory employing the capabilities of the Low Energy Radioactive Ion Beam Spectroscopy Station (LeRIBSS) [7, 20]. Radioactive nuclei were produced as fission fragments in a  $\text{UC}_x$  target using proton-induced fission of  $^{238}\text{U}$  and these nuclei were subsequently ionized in a hot-plasma ion source and extracted as a positive-ion beam. Following initial mass separation ( $\Delta M/M \sim 10^{-3}$ ) the ions were passed through a cesium-vapor charge-exchange cell to form a negative-ion beam. Since negative ions of zinc are not possible, this eliminates zinc as a contaminant in the beam. The beam was then tuned through the high-resolution isobar separator (nominally  $\Delta M/M \sim 10^{-4}$ ) for final beam purification before arrival at the experimental area. Isotopes of interest were delivered to the LeRIBSS which consists of a detector support (CARDS) and a fast-moving tape collector (MTC) with a tape transport time of 210 ms and a shielded tape storage volume. CARDS accommodated four HPGe clover  $\gamma$ -ray detectors and two plastic scintillators for  $\beta$ -particle detection situated around the beam pipe at the tape collection position. The clover array had a measured peak efficiency of 29% at about 100 keV and an efficiency of 5% at 1.33 MeV. All signals were processed using digital electronics [21].

The LeRIBSS is located just past the high-resolution

isobar separator which was used to select a purified  $^{75}\text{Cu}$  beam. This position allowed for an increased beam intensity due to bypassing the post-acceleration stage used in earlier experiments [22, 23] thus eliminating the factor of 10 loss in beam intensity from this step. The fact that acceleration is not required permits experiments with negative as well as positive ions at LeRIBSS. Positive ions have a factor of 10 smaller energy spread which allows for a much better isobaric separation [24]. The larger energy spread due to passage through the charge exchange cell reduces the effective resolution of the separator and leads to some  $^{75}\text{Ga}$  contamination in the beam. Since available rates were higher than we could effectively use, we narrowed the high resolution isobar separator image and object slits to obtain a beam of good purity with an average ion rate of  $> 2000$  ions/s.

An additional development was the installation of a rapid beam deflector upstream of the isobar separator allowing for a growth and decay MTC cycle (collect beam and measure, deflect beam and measure, and move) to be used. Due to the beam purification steps taken, the only significant contaminant was relatively long lived  $^{75}\text{Ga}$ . Given the half-lives of  $^{75}\text{Cu}$  (1.22 s),  $^{75}\text{Zn}$  (10.2 s), and  $^{75}\text{Ga}$  (126 s), an MTC cycle with a grow-in time of 5 s and a decay time of 7 s was used to minimize the effects of  $^{75}\text{Ga}$  accumulation. At this MTC cycle we could accumulate  $^{75}\text{Cu}$  ions to nearly the saturation point ( $5 \text{ s} \approx 4t_{1/2}$ ) and observe over a long decay time ( $7 \text{ s} \approx 5t_{1/2}$ ). Due to the passage through the charge exchange cell, there was no zinc in the beam, so it was produced entirely through the decay of copper. Since an enhanced purity beam was used, the buildup of the long-lived daughters was not a problem. However, the use of tape cycles helped us correctly identify  $\gamma$  rays associated with particular decays. Additional data were taken with the MTC stopped to obtain a saturation spectrum.

The overall run time was less than 3 hours including building saturation spectra. A representative  $\beta$ -gated spectrum from the saturation measurement is shown in Fig. 4. Analysis of the data resulted in 126  $\gamma$  transitions being assigned to the decay of  $^{75}\text{Cu}$  and allowed construction of the decay scheme shown in Figs. 5 and 6. Details of the decay scheme will be presented in the following section.

## III. EXPERIMENTAL RESULTS

### A. $^{75}\text{Cu}$ Half-life

The half-life of  $^{75}\text{Cu}$  was measured by observing the decay of the 109-, 193-, 268-, 345-, 421-, 476-, 724-, and 799-keV  $\gamma$  rays assigned to its decay and determined by taking the weighted average of all values obtained by fitting. The spectra were corrected by background subtraction. A plot of the decay curves for the selected  $\gamma$  rays as a function of time is shown in Fig. 7. The obtained half-life of 1.222(8) s is in good agreement with the pre-

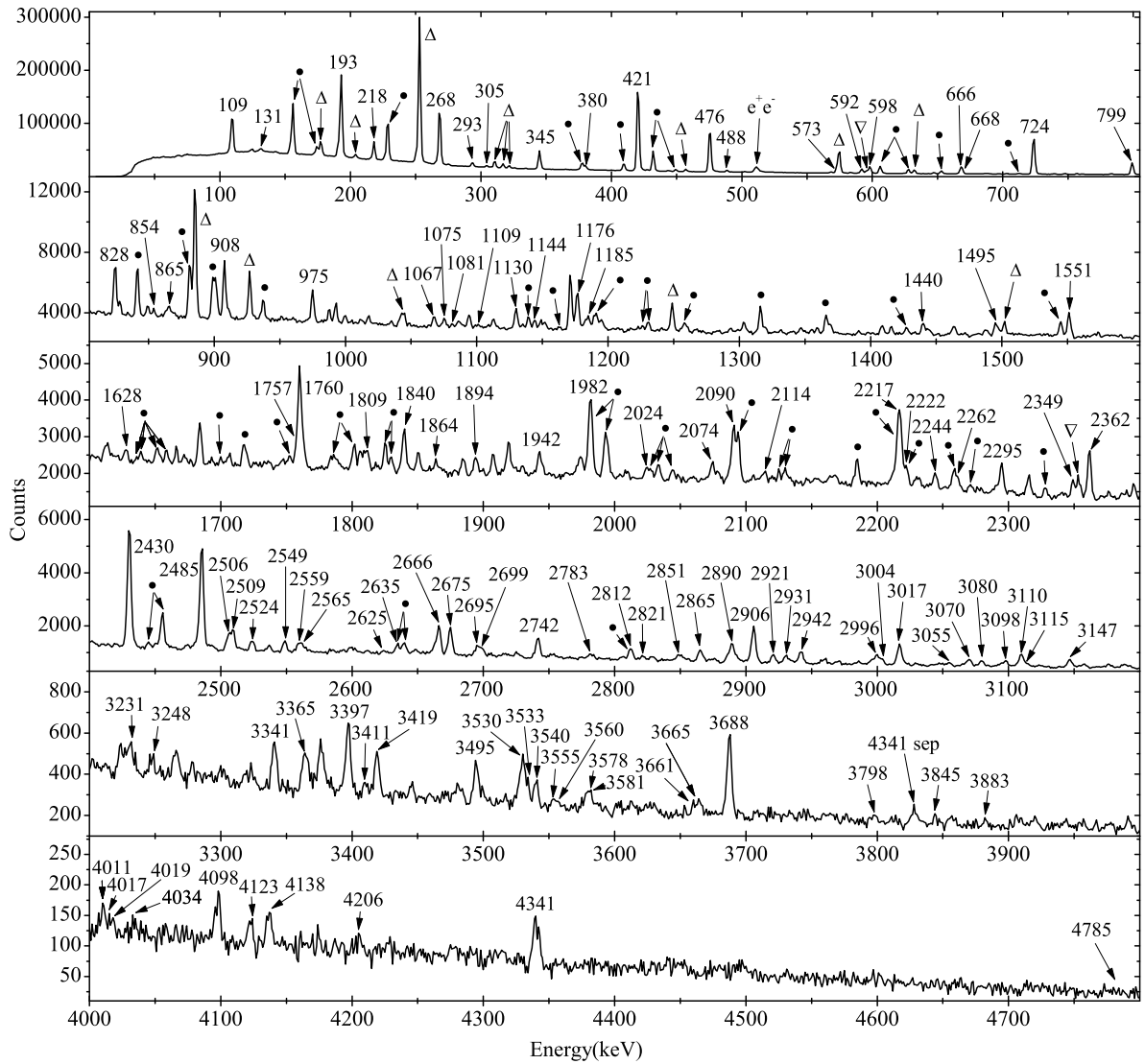


FIG. 4: Saturation spectrum obtained in the LeRIBSS data run with a purified  $^{75}\text{Cu}$  beam. The  $\gamma$ -ray peak, assigned to  $^{75}\text{Cu}$  are indicated by their energy with single and double escape peaks marked as sep and dep, respectively. Other members of the two decay chains are indicated by symbols:  $^{75}\text{Zn}$ ( $\bullet$ ),  $^{75}\text{Ga}$ ( $\Delta$ ),  $^{74}\text{Ga}$ ( $\nabla$ )

viously reported value of 1.224(3) s based on  $\beta$ -delayed neutron decay counting [10].

### B. Decay scheme development

The proposed decay scheme of  $^{75}\text{Cu}$  (Fig. 5 and 6) contains 59 levels including 120  $\gamma$  rays whose placements were made based on  $\gamma\gamma$  coincidence measurements. The  $\gamma$ -ray intensities are based on the analysis of  $\gamma$ -ray singles spectrum with the exception of a few weaker transitions. For these  $\gamma$  rays, analysis of a  $\beta$ -gated spectrum or a background subtraction technique were used. For the former case the  $\beta$ -detection efficiencies were estimated using stronger  $\gamma$  rays de-exciting the same level or levels

with about the same excitation energy. The obtained intensities are normalized relative to the 421-keV  $\gamma$  ray - the strongest transition observed in the decay - and corrected for summing effects. Most of the  $\beta$ -decay strength is concentrated up to  $\sim 1100$  keV and in the 3000-4000 keV range. Several transitions assigned to  $^{75}\text{Cu}$  decay have not been placed due to some ambiguity associated with them, and are reported in Table I. All  $\gamma$  rays with relative intensities greater than 1% have been placed in the proposed decay scheme or assigned to another decay. A number of unresolved doublets have been observed that have a component from  $^{75}\text{Zn}$  or  $^{75}\text{Ga}$   $\beta$  decay. These include the  $\gamma$  rays at 724, 855, 1552, 1982, 2217, 2222, 2350, 2635, and 2813 keV. The component of the intensity of these  $\gamma$  rays due to  $^{75}\text{Cu}$  decay was determined using

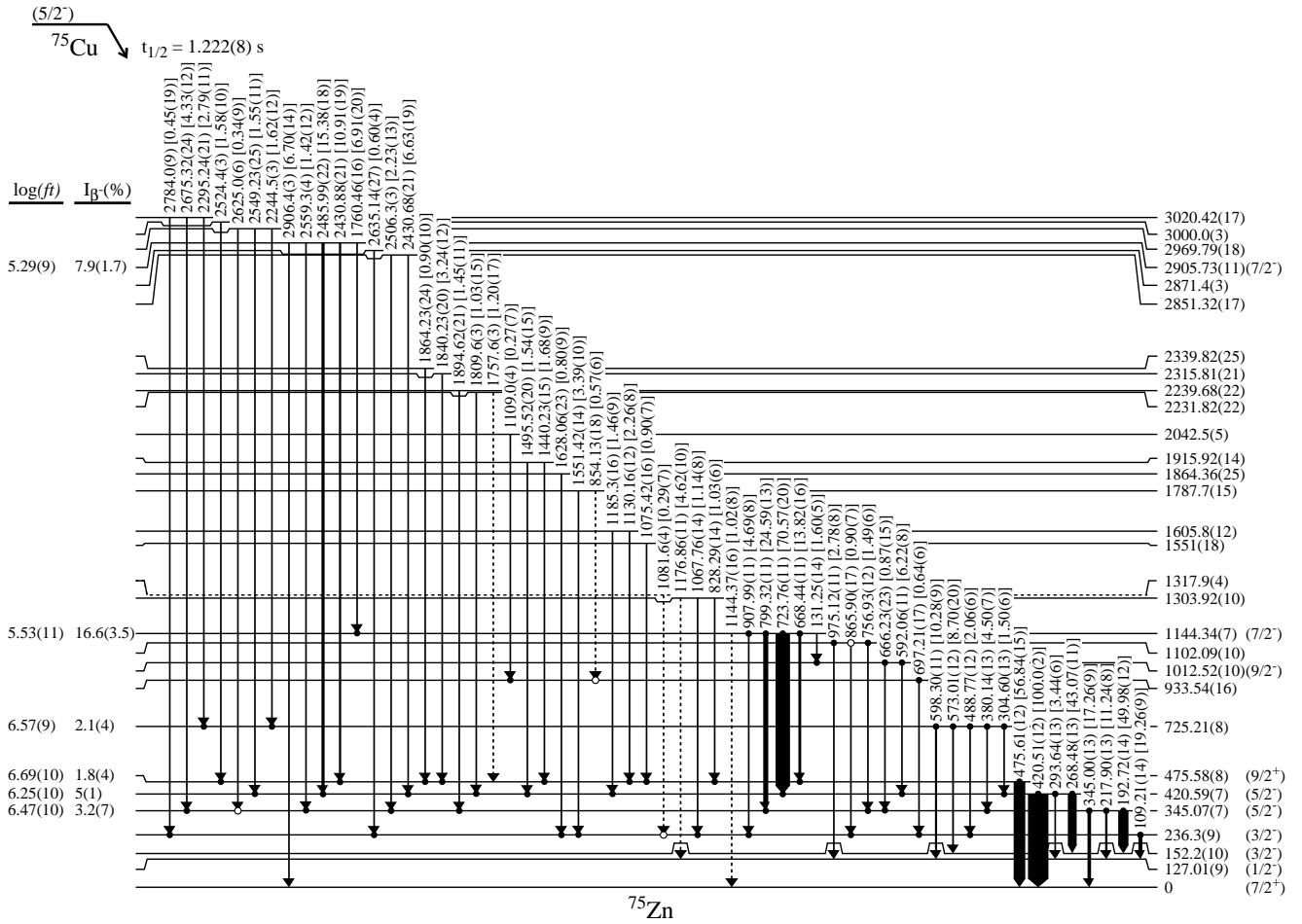


FIG. 5: Part I of the proposed decay scheme for  $^{75}\text{Cu}$  to excited states in  $^{75}\text{Zn}$  showing low energy transitions. The relative intensities of the  $\gamma$  rays to the 421-keV transition are indicated in the figure. Filled circles indicate  $\gamma$ - $\gamma$  coincidences seen both ways, whereas open circles indicate coincidences observed only from the upper transition. Transitions and levels without strong coincidence relationships and/or other linking transitions are indicated by dashed lines. The level feedings are based on an estimated absolute branching ratio of 19(4)% for the 421-keV transition, see text for details. Absolute  $\beta$ -decay feedings and  $\log ft$  values are specified for some levels. The  $\log ft$  values were calculated using mass values from Refs. [25] and [26].

saturation,  $\beta$ -gated and  $\gamma\gamma$  coincidence spectra.

The energy levels up to the 1144-keV level are established based on the following arguments. The 421-724-keV  $\gamma$ -ray sequence ordering is supported by the evidence that both  $\gamma$  rays are in coincidence with each other (Fig. 8) and the 421-keV transition is seen by many high-energy  $\gamma$  rays (Fig. 5 and 6) that in turn do not observe

the 724-keV  $\gamma$  ray thus putting the 724-keV  $\gamma$  ray above the 421-keV  $\gamma$  ray, thus establishing the 1144-keV level. The 668-724-799-908-keV group was assigned to depopulate the same 1144-keV level because all of these transitions are seen by a 1760-keV  $\gamma$  ray (Fig. 8) and many other higher-energy  $\gamma$  rays and they are not in coincidence with each other (e.g. the 724- and 799-keV gates in Fig. 8). These transitions lead to additional levels at 236, 345, and 476 keV. The 1144-keV  $\gamma$  ray is dashed because its energy matches that for a cross-over transition to the ground state but it is not seen in coincidence with any other  $\gamma$  rays.

The  $\gamma$  rays at 193, 218, and 345 keV are observed by the 799-keV  $\gamma$  ray (Fig. 8) and numerous higher-energy  $\gamma$  rays that all see the same sequence of  $\gamma$  rays in their coincidence gates. These three  $\gamma$  rays are not observed to be in coincidence with each other. Furthermore, the energy separation between these  $\gamma$  rays exactly matches that of

TABLE I: Unplaced  $\gamma$  rays associated with  $^{75}\text{Cu}$  decay.

Energy (keV)	$I_{\gamma(\text{rel})}$ <sup>a</sup> (%)	Energy (keV)	$I_{\gamma(\text{rel})}$ <sup>a</sup> (%)
4011.5(7)	0.3(6)	4017.0(6)	< 0.2
4019.0(6)	< 0.2	4098.4(5)	0.6(1)
4137.7(5)	0.5(1)	4206.3(9)	0.2(1)

<sup>a</sup>Relative to the 421-keV  $\gamma$  ray.



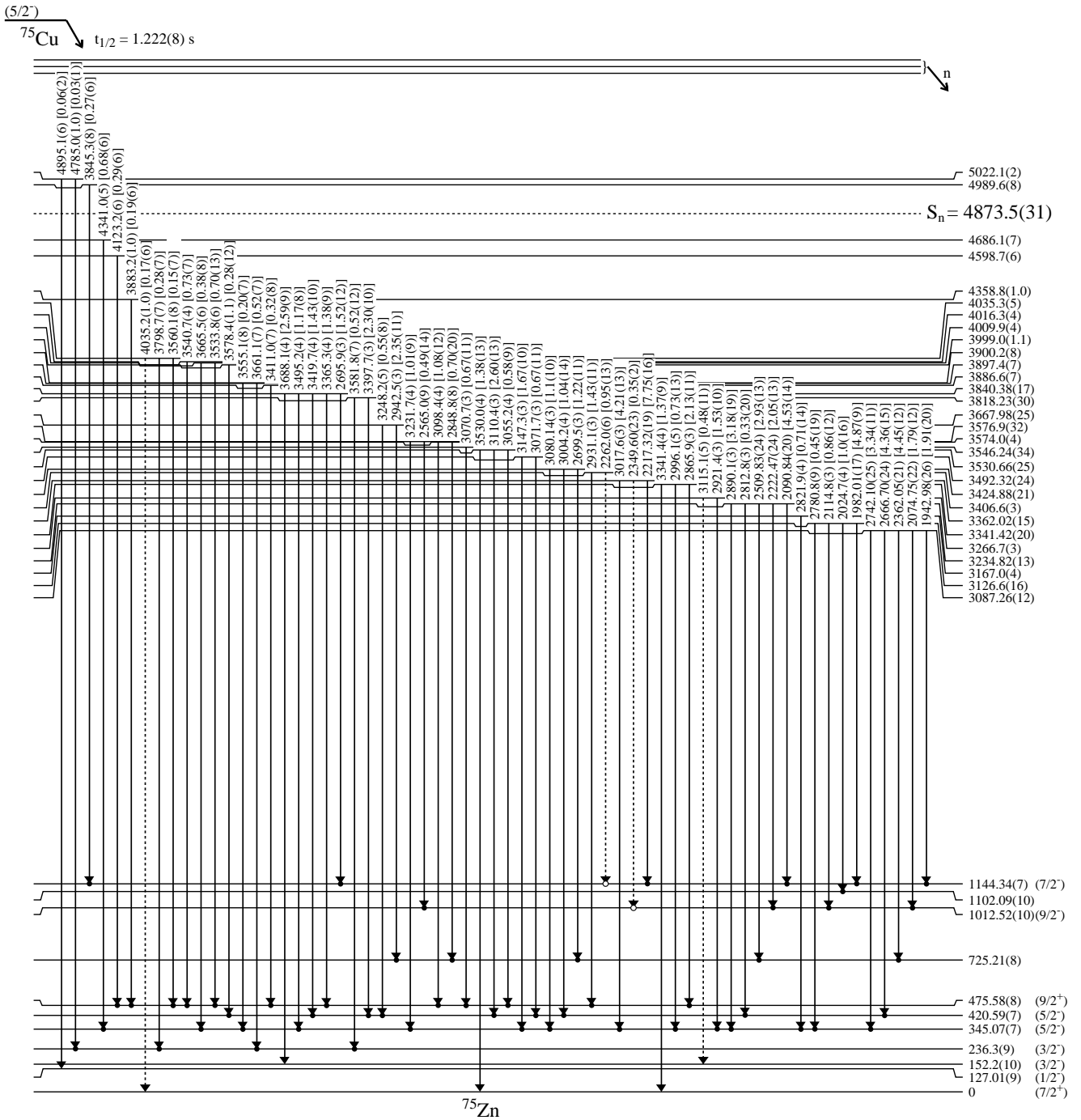


FIG. 6: Part II of the proposed decay scheme for  $^{75}\text{Cu}$  to excited states in  $^{75}\text{Zn}$  showing high energy transitions. The relative intensities of the  $\gamma$  rays to the 421-keV transition are indicated in the figure. Filled circles indicate  $\gamma$ - $\gamma$  coincidences seen both ways, whereas open circles indicate coincidences observed only from the upper transition. Transitions and levels without strong coincidence relationships and/or other linking transitions are indicated by dashed lines.

the 268-, 294-, and 421-keV  $\gamma$  rays observed in the 724-keV coincidence gate. Finally, this latter set of three  $\gamma$  rays are also not observed to be in coincidence with each other. Therefore, the 193-218-345 group de-exciting the 345-keV level and the 268-294-421 group de-exciting the 421-keV level establish levels at 127, 152, and 345 keV.

In a search for  $\gamma$  rays at 127- and 152-keV, both singles and  $\gamma\gamma$  coincidence spectra were investigated. However, no evidence for  $\gamma$  rays at these energies was observed suggesting that there is no direct link between these states and the ground state.

The 908-109 sequence is the third cascade originating

from the 1144-keV level. This cascade fits in the decay scheme providing additional support for the existence of the 127-keV level. The order of the  $\gamma$  rays in this cascade is based on the large number of coincident transitions observed in the 109-keV gate while only the two  $\gamma$  rays at 109- and 1760-keV are observed in the 908-keV gate. This establishes the level at 236 keV.

Placement of the 476-keV transition was complicated by the fact that it is not in coincidence with any other major  $\gamma$  ray and the peak at 668 keV seen in the 476-keV coincidence gate (Fig. 8) is interpreted as being representative of two different  $\gamma$  rays with part of it being in coincidence with the 193-218-345 group. If the 668-keV peak represented only a single transition, the strong coincidences with the 193-keV peak seen in Fig. 8 could only be accounted for if a third linking transition of about 130-keV energy depopulating the 476-keV state were present. A 131-keV transition does exist in the spectrum (Fig. 4) and it is observed to be in coincidence with a 666-keV  $\gamma$  ray. However, it is assigned to de-excite the 1144-keV state based on  $\gamma\gamma$  coincidences with a 421-592 cascade. It could thus be concluded that the peak near 668-keV is in fact composed of two different  $\gamma$  rays at 666 and 668 keV. Coupling this result with numerous high-energy  $\gamma$  rays in the 476-keV coincidence gate and the presence of the 666-keV  $\gamma$  ray in the 193-keV gate (see Fig. 8) allows the definite placement of levels at 476- and 1013-keV in the decay scheme.

The assumption that four cascades – 908-109, 799-(193,218,345), 724-(268,294,421), and 668-476 – are in parallel is supported by the fact that no coincidences are observed between  $\gamma$  rays in one cascade and any other

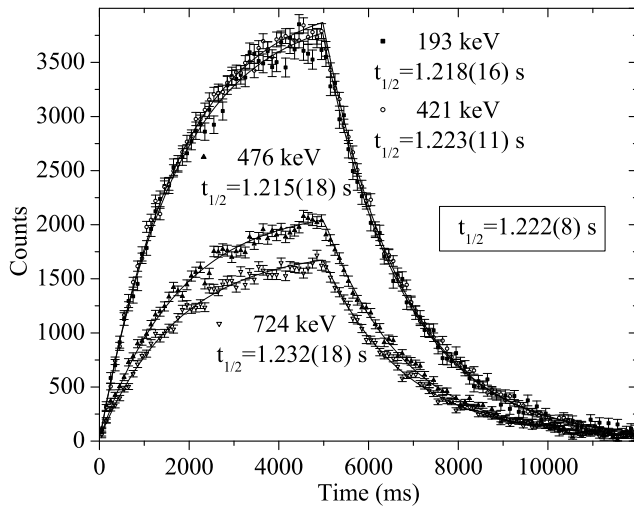


FIG. 7: Half-life curves for  $\gamma$  rays depopulating the 193-, 421-, 476-, and 724-keV levels. Data were fit in both the growth and the decay portions of the curve, to optimize statistics, using a nonlinear least-squares fit routine. The average half-life value was determined from the half-life values for the 109-, 193-, 268-, 345-, 421-, 476-, 724-, and 799-keV transitions.

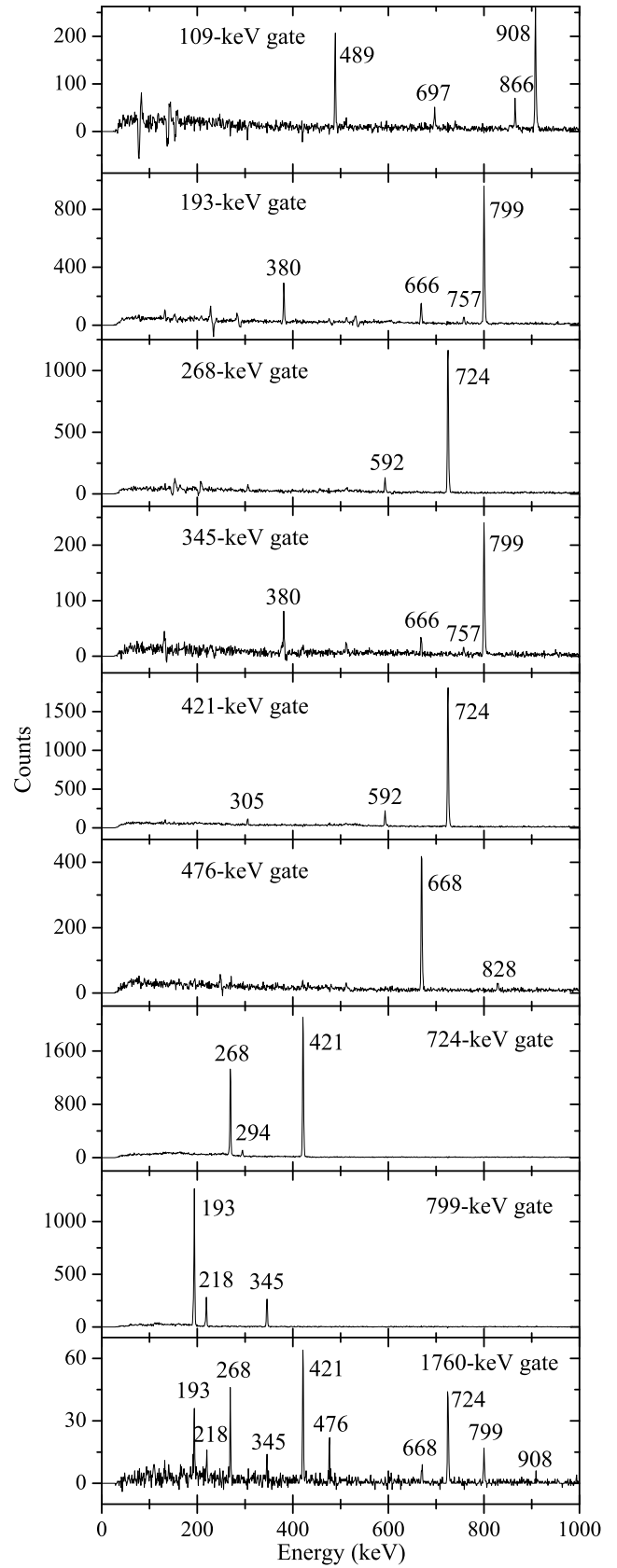


FIG. 8:  $\gamma$ -ray spectra coincidence with the 109-, 193-, 268-, 345-, 421-, 476-, 724-, 799-, and 1760-keV transitions.

cascade from the 1144-keV level (Fig. 8).

It is apparent in Fig. 8 that the 489-keV  $\gamma$  transition is in coincidence with the 109-keV  $\gamma$  ray. From the coincidence relationships for the 489- and 598-keV  $\gamma$  rays with higher energy  $\gamma$  rays and the fact that the energy sum for the 489-109 cascade is equal to 598-keV suggests that the 489 and 109-keV coincident radiations are adjacent in the cascade and that the 598-keV  $\gamma$  ray represents the crossover transition. A similar argument holds for the 380-keV transition populating the 345-keV level and provides evidence for placement of the 573-keV  $\gamma$  ray. These cascades combine to establish the level at 725 keV.

The levels at 934 and 1102 keV are established by the strong coincidences between the 109-keV  $\gamma$  ray and  $\gamma$  rays at 697 and 866 keV (Fig. 8). The 697-keV  $\gamma$  ray also has a strong coincidence with an 1109-keV  $\gamma$  ray. However, the latter cannot be used in establishing the level at 934 keV due to lack of a cross-over transition from the 2042-keV state. Placement of the 1102-keV level is confirmed by the 757-keV  $\gamma$  ray observed in the 193-keV gate.

All levels in the decay scheme above 1144-keV are observed to decay only to states at or below this level. The levels are all established by  $\gamma\gamma$  coincidence relationships observed in both the gate on the  $\gamma$  ray de-exciting the level and gates on the  $\gamma$  rays below this in the proposed decay scheme. Any  $\gamma$  rays feeding into the 236-keV level or above but which are not confirmed by coincidences being observed both ways are dashed in the decay scheme. A number of  $\gamma$ -ray transitions placed in the decay scheme populate the ground, 127-, and 152-keV states but are considered to be well established by their observed relative intensity being greater than 1% as well as a good energy match as a crossover transition. None of these  $\gamma$  rays are observed to be in coincidence with any of the  $\gamma$  rays placed in the lower portion of the decay scheme.

### C. Levels above the neutron separation energy

Three  $\gamma$  rays are observed to de-excite two levels (4990 and 5022 keV) above the neutron separation energy at  $S_n = 4874(3)$  keV ([15]). Both the 3845- and 4785-keV  $\gamma$  rays are established by convincing coincidence relations (see Fig. 9). The 4895-keV  $\gamma$ -ray placement is based on energy matching as a cross-over transition and lack of  $\gamma\gamma$  coincidences even though it is more intense than the 4785-keV  $\gamma$  ray.

The establishment of two  $^{75}\text{Zn}$   $\gamma$ -decaying states above the neutron separation energy and a similar observation of three states in  $^{77}\text{Zn}$  [7] may have an effect on theoretical calculations of  $\beta$ -delayed neutron branching ratios in this nuclear mass range. Currently, the calculations are typically being done under the assumption of a two-way  $\beta$ -strength distribution - with a sharp cut above and below the neutron separation energy. The fact that we identified levels lying above the neutron separation energies which decay at least partially by  $\gamma$  emission, not entirely by  $\beta$ -delayed neutron emission, suggests that the previ-

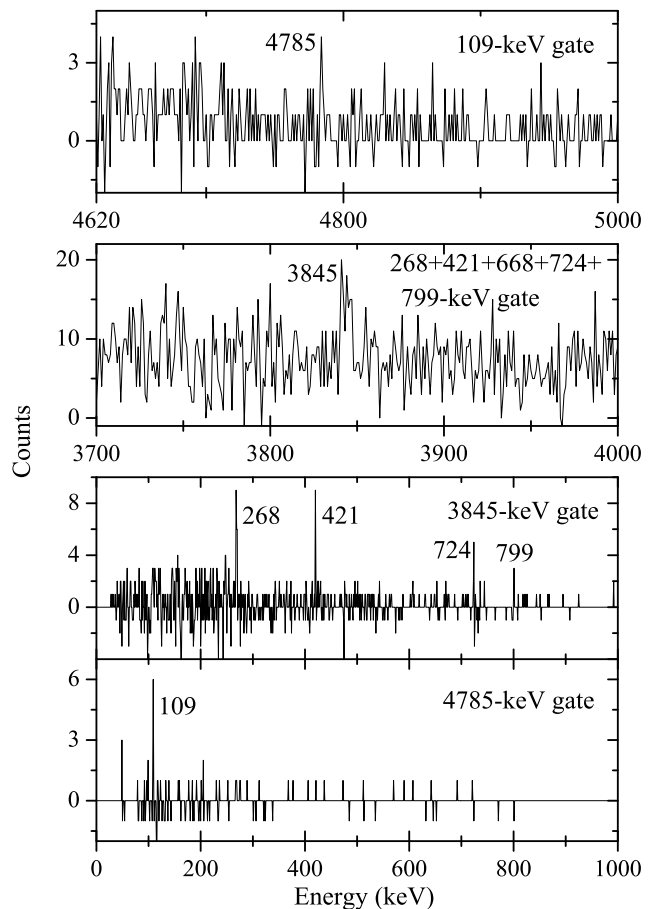


FIG. 9: Portions of the  $\gamma$ -ray coincidence spectra for the 109-, 268+421+668+724+799-, 3845-, and 4785-keV transitions.

ous assumption might not be valid and more comprehensive theoretical analysis of  $\beta$ -delayed neutron branching ratios is needed.

### D. Estimation of absolute branching ratios

The absolute branching ratio of the 421-keV  $\gamma$  ray could not be directly determined in this experiment. A comparison to the known decay scheme for  $^{75}\text{Ga}$  was not possible because of the unknown amount of primary gallium in the beam. In addition, we cannot use the published absolute branching ratio for  $^{75}\text{Zn}$  decay since we do not know the effect of the feeding through the 127- and 152-keV levels on this value. However, a range of values can be given based on information available from the decay scheme obtained as described in the following paragraphs. Although we do not observe a transition between the 152- and 127-keV levels since this energy (25 keV) is below our energy threshold, we will assume this transition does exist as will be argued later. In addition, some of the arguments will be based upon spin/parity assignments which will be presented later.

First, we assume that we have observed all the  $\gamma$ -ray intensity from the decay and there is no direct feeding to the ground state, or 127- and 152-keV levels (Fig. 10(a)). This assumption is not completely correct as there should be some direct feeding to the ground state since this is a first forbidden transition (the  $5/2^-$   $^{75}\text{Cu}^g$  to the  $7/2^+$   $^{75}\text{Zn}^g$ ), any direct feeding to the 127- and 152-keV levels cannot be measured, and any intensity from  $\gamma$  rays feeding into these states would result in an increase in the total  $\beta$ -decay intensity. Therefore, this assumption imposes the absolute upper limit since any missing feeding will reduce the value. Based on the published value of 96.5(6)% for the  $\beta$ -decay branching ratio [11], we obtain an upper limit of 28.3(2)% for the absolute branching

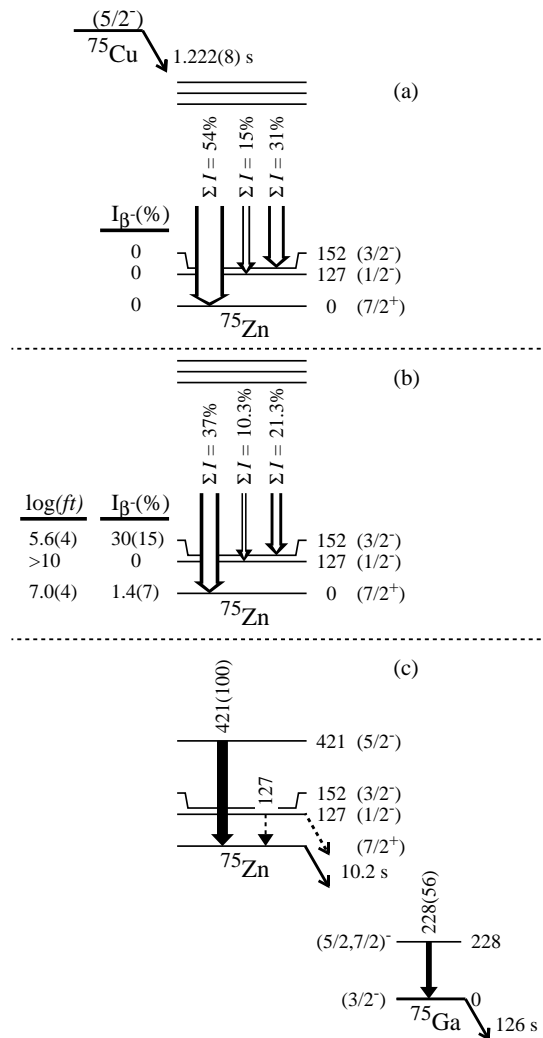


FIG. 10: Different scenarios of  $\beta$  decay of  $^{75}\text{Cu}$  to levels in  $^{75}\text{Zn}$  used to determine the limits for the absolute branching ratio of the 421-keV  $\gamma$  ray transition. The sum relative  $\gamma$ -ray intensities (the actual value of 353 was normalized to 100%) to corresponding levels are represented by white arrows and absolute  $\beta$  intensities are shown traditionally on the left next to energy levels. (See text for details.)

ratio of the 421-keV  $\gamma$  ray.

Second, we can refine the previous estimate by considering possible unobserved direct feeding. As mentioned above, the actual feeding will be lower since it is not unlikely that there exists some unobserved branching to the ground state from the high energy states or unobserved direct feeding to the three lowest energy states in  $^{75}\text{Zn}$ . Unobserved feeding from higher-lying states (above 2 MeV) is probably insignificant since it would likely feed through observed transitions and not go directly to one of the three lowest states. To determine the effect of the unobserved feeding to the three lowest states, we estimated this feeding based on the spin/parity assignments presented later. There should be no substantial feeding to the proposed 1/2<sup>-</sup> isomeric state at 127 keV as it would require a second forbidden transition ( $5/2^- \rightarrow 1/2^-$ ). If we then assume reasonable  $\log ft$  values of 5.6(4) for allowed feeding to a 3/2<sup>-</sup> 152-keV state and 7.0(4) for first-forbidden feeding to the 7/2<sup>+</sup> ground state, we would estimate the unobserved  $\beta$  feeding to be 30(15)% and 1.4(7)%, respectively (Fig. 10(b)). These values can be used to obtain a more realistic estimate of 19(4)% for the 421-keV absolute branching ratio.

Third, we can assume that there is an unobserved linking transition between the ground and the first excited states (Fig. 10(c)) and get an estimate on the absolute branching ratio of the 421-keV  $\gamma$  ray by direct comparison to  $\gamma$  rays from  $^{75}\text{Zn}$   $\beta$  decay. The basic assumption is that all the feeding goes through the ground state and the measured absolute branching ratio for the 228-keV  $\gamma$  ray from  $^{75}\text{Zn}$  (28.9(14)%) [18] can be used directly. The value obtained by this analysis is 49.8(25)% when considering the  $^{75}\text{Cu}$   $\beta$ -branch value of 96.5(6)%. This value which exceeds our previously established upper limit, indicates that the 1/2<sup>-</sup> state has a significant  $\beta$ -decay branch thus confirming the existence of an isomeric state.

Finally, we assume a 100%  $\beta$ -decay branch from the 1/2<sup>-</sup> isomeric state which directly feeds the  $^{75}\text{Zn}$  ground state, keep the assumptions about direct feeding to the three lowest states, and again do the direct comparison between the 421- and 228-keV  $\gamma$  rays. The resulting absolute branching ratio for the 421-keV transition is 19(4)%. The agreement between this value and that obtained from the total intensity sum using the same assumptions about unobserved direct feeding suggests that a value of 19(4)% is a reasonable estimate. We chose to use this for the determination of the level feedings and  $\log ft$  values shown in Fig. 5.

### E. $\beta$ -delayed neutron branching ratio

The  $\beta$ -delayed neutron branching ratio of  $^{75}\text{Cu}$  could not be determined from the ratio of corresponding  $\gamma$ -ray intensities. The problem is related to the difficulty in extracting meaningful values for both the  $\beta$  and  $\beta n$  branches (Fig. 11). As mentioned in the previous sec-

tion, the unknown absolute branching ratio for the 228-keV transition in  $^{75}\text{Ga}$  fed by  $\beta$  decay and  $^{75}\text{Ga}$  in the beam make the  $P_n$  determination using the  $\beta$  branch impossible. In addition, our experimental setup did not allow us to measure directly the exact number of  $^{75}\text{Cu}$  ions in the beam, so that a determination using only the  $\beta n$  branch is not possible. The presence of  $^{74}\text{Zn}$  is confirmed by the 606-812-keV cascade but since the energies of the  $\gamma$  rays from the decay of  $^{74}\text{Zn}$  are fairly low, their intensities could not be accurately determined due to a high background level. Therefore, we have used the previously reported value of 3.5(6)% [11] since systematics in this region [22] indicate that this value is reasonable.

### F. Spin-parity assignments for levels in $^{75}\text{Zn}$

The arguments in the Sec. III B establish the primary low-energy level structure of  $^{75}\text{Zn}$ . Based on the present level arrangement, it is now possible to make predictions concerning the spin-parity assignments for some of these states.

The ground state of  $^{75}\text{Zn}$  was deduced in its  $\beta$  decay study [18] based on the following arguments. It was found experimentally [18] that the decay patterns of  $^{75}\text{Zn}$  and  $^{77}\text{Zn}$  are very similar with the maximum of the  $\beta$ -strength centered near 2.5 MeV in the gallium nuclei.  $J^\pi = 7/2^+$

was assumed [18] to be the ground state of  $^{77}\text{Zn}$  similar to that of  $^{77}\text{Ge}$  [27]. Therefore, a  $J^\pi$  of  $7/2^+$  has been adopted for the ground state of  $^{75}\text{Zn}$  as well. Low-lying  $7/2^+$  states in this area of the nuclear chart have been interpreted as being due to a  $(g_{9/2})^3$  configuration rather than the  $g_{7/2}$  single-particle state [28]. A splitting between the  $^{77}\text{Ge}^g$ , if assumed to be a  $g_{7/2}$  single-particle state, and a  $g_{9/2}$  second excited state would be too small to be compatible with the much larger energy separation required by spin-orbit coupling [29]. Therefore, it seems likely that these levels can be thought of as arising from the coupling of an odd nucleon and a Coriolis-broken pair of nucleons all adding their spins together.

One particular feature of the  $^{75}\text{Zn}$  structure is that there are two low-lying levels sitting close to each other at 127 and 152 keV which do not appear to have  $\gamma$  rays de-exciting them. For  $\beta$  decay to compete with an IT transition of 25 or 152 keV, a multipolarity of M2 as the lowest multipolarity exit channel is needed. This can only happen if  $J^\pi = 11/2^-$ , an improbable situation given the orbitals available. It is, therefore, unlikely that  $^{75}\text{Zn}$  will have two  $\beta$  decaying isomers. Consequently, similar to other cases in this nuclear mass range, we have assumed that  $^{75}\text{Zn}$  has a single  $\beta$ -decaying isomeric state. The assumption of a low-energy 25-keV highly converted M1 transition between the 152- and 127-keV levels seems quite reasonable. This energy is below our detection limit and additional specifically designed conversion electron measurements would be needed to confirm this suggestion.

From systematics, the first excited isomeric state at 127 keV could reasonably be assigned to be  $1/2^-$  since this type of isomerism is expected to occur (see Figs. 2 and 3). The reason why the isomeric state has not been observed previously is because it might predominantly feed directly the  $3/2^-$   $^{75}\text{Ga}^g$  and thus cannot be seen among  $\gamma$ -ray transitions belonging to  $^{75}\text{Zn}$  decay in a manner similar to that known in the  $\beta$  decay of  $^{77}\text{Zn}$  [7]. This conjecture is supported by the results of our absolute branching ratio estimate where this assumption was used. In this arrangement with  $J^\pi = 7/2^+$  and  $1/2^-$  being the ground and the first excited states, respectively, the allowed  $\beta$  transition from  $1/2^-$   $^{75}\text{Zn}^m$  to the  $J^\pi = 3/2^-$  ground state of  $^{75}\text{Ga}$  would bypass the 228-keV transition in  $^{75}\text{Ga}$ . The non-observation of a 127-keV  $\gamma$  ray can also be understood from the systematics (Fig. 3). For  $^{79}\text{Se}$  and higher- $Z$   $N = 45$  isotones, the  $1/2^-$  isomer decays to the  $7/2^+$  ground state by a 100% IT branch. At  $^{77}\text{Ge}$ , the increase in the  $\beta$ -decay energy allows a competition between the two decay paths such that an 81%  $\beta$ -decay branch occurs [15]. With the further increase in available  $\beta$ -decay energy at  $^{75}\text{Zn}$ , it is reasonable to assume that the  $\beta$ -decay branch will reach nearly 100%. The Weisskopf estimate for a 127-keV E3 transition is 6.8 s, so an allowed  $\beta$  decay to low-spin negative parity states in  $^{75}\text{Ga}$  should be the dominate decay path.

Based on the assignments of the spin/parity of

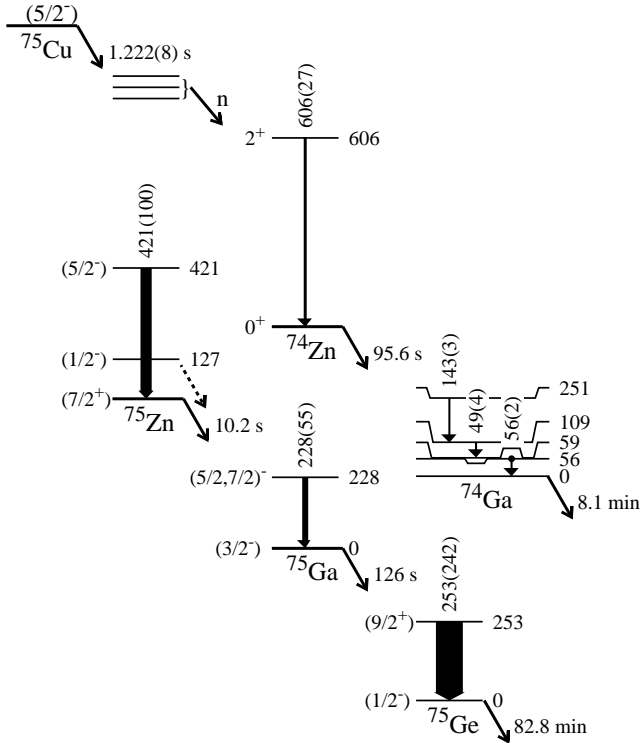


FIG. 11: Subset of the decay schemes of  $^{75}\text{Cu}$  and its daughter activities used to estimate the  $P_{\beta n}$  value. The intensities shown are relative to the 421-keV transition.

the ground and isomeric states, we can make further spin/parity assignments for additional levels based on their decay patterns to these states (see Figs. 5, 6, and Table II). These assignments will be based on a few simple assumptions. First, it is assumed that only  $\gamma$  rays with multiplicities of E1, M1/E2, or E2 will be observed. Any higher multipolarity transitions are improbable since a lower multipolarity transition should be possible to either the ground or isomeric state. This assumption will limit the spin/parity assignment for a number of levels to only a few possibilities. Second, we will assume that in general the dipole transitions will be stronger. This is not a firm requirement since the actual wave functions will determine the transition probability, but does provide some guidance. Third, additional insight is provided by considering the strength of the  $\beta$ -decay feeding to the level. The  $\pi 1f_{5/2}$  ground state of  $^{75}\text{Cu}$  will feed  $3/2^-$ ,  $5/2^-$ , and  $7/2^-$  states by allowed transitions, and  $3/2^+$ ,  $5/2^+$ , and  $7/2^+$  states by first forbidden transitions. Any feeding to a  $9/2^+$  state will be a very weak first forbidden unique  $\beta$  decay. These last two assumptions will suggest a preferred assignment from the values specified by the first assumption.

The strongest  $\gamma$  ray in the decay links the 421-keV state to the  $7/2^+$   $^{75}\text{Zn}$  ground state. This level also has a much weaker transition, 294 keV, to the  $1/2^-$  isomeric state. This observation with a difference of three units of angular momentum and a change in parity requires one transition to be of E1 multipolarity while the other is of E2 multipolarity, and limits the spin/parity assignment to  $3/2^+$  or  $5/2^-$ . The much greater intensity for the 421-keV  $\gamma$  ray favors it being the E1 transition in the pair. Therefore, we suggest a  $J^\pi = 5/2^-$  for the 421-keV state. The apparent  $\beta$ -decay feeding to this level with  $\log ft = 6.3(3)$  is consistent with either an allowed or first-forbidden decay. Arguments to firm up the assignment for this level will be presented later.

The 476-keV level de-excites by a single  $\gamma$  ray transition to the ground state. This single transition cannot put a strong limit on the spin/parity assignment. However, the lack of observed transitions to the isomeric state and the 421-keV level can be used to restrict the assignment. If the 421-keV level is  $5/2^-$  then the spin/parity is restricted to  $9/2^+$ . However, if the 421-keV level is a  $3/2^+$  state then  $7/2^-$  and  $9/2^-$  assignments are also possible. From systematics of the  $N = 45$  isotones (Fig. 3) we expect to observe a low-lying  $9/2^+$  state. The energy separation between this state and the  $7/2^+$  ground state appears to be increasing in energy as  $Z$  decreases, so an energy separation of 476 keV is reasonable. No other observed state has a decay pattern which would suggest a  $9/2^+$  assignment. Therefore, although based on the non-observation of transitions, we assume this assignment is  $9/2^+$  and will consider this a firm assignment for later arguments.

The 1144-keV level is observed to de-excite by strong transitions to the 421- and 476-keV levels, a weak possible transition to the ground state, and no transition

to the isomeric state. In addition, it is observed to be the strongest directly fed state in  $\beta$  decay resulting in an apparent  $\log ft$  value of 5.6(4). Although not conclusive, this result is indicative of an allowed  $\beta$  decay which limits the spin/parity to  $3/2^-$ ,  $5/2^-$  and  $7/2^-$ . This assignment can further be restricted to  $7/2^-$  by the lack of a transition to the isomeric state. A first-forbidden  $\beta$  decay to this state cannot be ruled out, but this would mean there are no states fed by allowed  $\beta$  decays. This value also restricts the assignment for the 421-keV level to  $5/2^-$  as previously suggested. A  $5/2^-$  assignment for the 421-keV level adds further support to a  $9/2^+$  assignment for the 476-keV level since the two negative parity possibilities should have resulted in an observed transition to the 421-keV level.

The 2906-keV level also exhibits strong  $\beta$  feeding indicating an allowed transition which limits its spin/parity to  $3/2^-$ ,  $5/2^-$ , and  $7/2^-$ . This level is observed to connect by  $\gamma$ -ray transitions to  $5/2^-$ ,  $7/2^\pm$ , and  $9/2^+$  levels which limits the assignment to  $7/2^-$ . This assignment is further justified by the observation that the strongest transition, 2486 keV, is to the  $5/2^-$  421-keV level indicating a strong M1 transition.

The 345-keV level has a decay pattern similar to the 421-keV level which restricts the spin/parity assignment to  $3/2^+$  or  $5/2^-$ . The major difference is in the intensity of the decay pattern which suggests a difference in the structure of the states. The 218- and 345-keV transitions are of about equal intensity, while the 193-keV transition to the 152-keV level is the strongest. We might then assume that the 345- and 421-keV levels do not have the same spin/parity assignment. However, the 799-keV  $\gamma$  ray from the 1144-keV level requires a  $5/2^-$  assignment. The observed  $\beta$ -decay feeding and  $\log ft$  values are consistent with either allowed or first forbidden  $\beta$  decays, so no distinction based on this is possible. Yet, the nearly identical  $\beta$ -decay feeding to these states suggests that they must be fed by the same type of  $\beta$  decay lending support to the  $5/2^-$  assignment for the 345-keV level. The hinderance of the E1 transition to the ground state would be an indication of significant differences in the structure of the two states.

A spin/parity assignment for the 152-keV level requires considering the transitions feeding it from the 345-, 421-, and 1144-keV levels as well as the lack of a transition to the ground state. The requirement of no feeding to the ground state limits the possible assignments to  $1/2^-$  and  $3/2^-$ . This assignment is further restricted to be  $3/2^-$  by the observed transition from the 1144-keV state. This assignment is also consistent with the  $5/2^-$  assignments for the 345- and 421-keV levels which show strong E1 and M1/E2 transitions to the ground state and 152-keV level, respectively, and a weaker E2 transition to the isomeric state.

The 236-keV level has  $\gamma$ -ray transitions connecting it to  $1/2^-$  and  $7/2^-$  states. This observation restricts the spin/parity assignment to be  $3/2^-$  or  $5/2^-$ . The weaker intensity of the 908-keV transition out of the 1144-keV

level compared to the dipole transitions suggests that this might be of E2 multipolarity. In addition, the lack of observed transitions to the ground state or 152-keV level suggest that the 109-keV transition must be a dipole transition. Therefore, we favor a  $3/2^-$  assignment for this state.

The 1013-keV level does not have any apparent  $\beta$ -decay feeding, has observed  $\gamma$ -ray transitions connecting it to  $5/2^-$  and  $7/2^-$  states, and no observed transitions to the  $1/2^-$ ,  $3/2^-$ ,  $7/2^+$ , and  $9/2^+$  states. If we consider only the observed transitions, the lack of direct  $\beta$  feeding suggests a  $9/2^-$  assignment, requiring a strong hinderance of the E1 transitions to the ground state and 476-keV level.

Similar arguments based on the observed  $\gamma$  ray decay patterns of the levels connected to by each level can be made. The results of this analysis, using the previously discussed spin/parity assignments, are presented in Table II. In this analysis, only observed  $\gamma$ -ray transitions were considered. In addition, for levels above 1144 keV, direct feeding in the  $\beta$  decay requires allowed or first-forbidden  $\beta$  decays which limits the spin/partity assignments to  $3/2^\pm$ ,  $5/2^\pm$ , and  $7/2^\pm$ . However, it is not possible to distinguish between these two modes of  $\beta$  decay. Only cases which are limited to four or fewer possible assignments are shown in Table II.

Identification of the proposed lowest  $1/2^-$  and  $9/2^+$  states in  $^{75}\text{Zn}$  allows us to complete the systematics for evolution of these states up to  $N=47$  in the odd-A zinc isotopes (Fig. 12). The energy of the  $1/2^-$  isomer follows

TABLE II: Proposed spin/parity assignments for selected levels in  $^{75}\text{Zn}$ .

Level Energy (keV)	$J^\pi$ Connected Levels	Proposed $J^\pi$ Assignment
725	$1/2^-, 3/2^-, 5/2^-$	$3/2^\pm, 5/2^\pm$
1102	$1/2^-, 5/2^-$	$1/2^-, 3/2^\pm, 5/2^-$ <sup>a</sup>
1304	$3/2^-, 9/2^+$	$5/2^+, 7/2^-$
1606	$5/2^-, 9/2^+$	$5/2^+, 7/2^\pm$
1916	$5/2^-, 9/2^+$	$5/2^+, 7/2^\pm$
2232	$5/2^-, 9/2^+$	$5/2^+, 7/2^\pm$
3087	$5/2^-, 7/2^-, 9/2^-$	$5/2^-, 7/2^\pm$ <sup>b</sup>
3127	$5/2^-, 7/2^-, 9/2^-$	$5/2^-, 7/2^\pm$
3235	$5/2^-, 7/2^-, 9/2^-$	$5/2^-, 7/2^\pm$ <sup>b</sup>
3341	$5/2^-, 7/2^+, 9/2^+$	$5/2^+, 7/2^\pm$
3362	$5/2^-, 7/2^-, 9/2^-$	$5/2^-, 7/2^\pm$ <sup>b</sup>
3531	$5/2^-, 7/2^+, 9/2^+$	$5/2^+, 7/2^\pm$
3362	$5/2^-, 9/2^-$	$5/2^-, 7/2^\pm$
3840	$3/2^-, 5/2^-, 7/2^-, 9/2^+$	$5/2^+, 7/2^\pm$ <sup>b</sup>
4010	$5/2^-, 9/2^+$	$5/2^+, 7/2^\pm$
4035	$3/2^-, 7/2^+, 9/2^+$	$5/2^+, 7/2^-$

<sup>a</sup>The weak  $\beta$ -decay feeding suggest a first forbidden decay limiting the assignment to  $3/2^+$ .

<sup>b</sup>Strong  $\beta$ -decay feeding suggests an allowed decay which would allow rejection of positive parity states. However, the  $\log ft$  value is inconclusive.

the expected trend for the zinc isotopes, but has a lower energy than would have been expected from the systematics of the odd-A  $N=45$  isotopes (Fig. 3). Conversely, the  $9/2^+$  state follows the expected trend from the  $N=45$  isotopes, but is at a much higher energy than expected when comparing to this state in  $^{77}\text{Zn}$ .

#### IV. DISCUSSION

The observed structure of  $^{75}\text{Zn}$  is similar to that of both the other zinc isotopes as well as the  $N = 45$  isotones. However, there is a significantly larger number of low spin, negative parity states at low energy in  $^{75}\text{Zn}$  when compared to these other nuclei. The question then arises as to the composition of these states. As a first step, consider the possible states which can arise from simple shell model arguments. The positive parity states come from the  $(\nu g_{9/2})^3$  couplings. As mentioned previously, the ground state is understood to come from a three-quasiparticle configuration [18], while the  $9/2^+$  state is probably composed of both single-particle and three-quasiparticle configurations. The presence of negative parity states requires breaking the  $\nu p_{1/2}$  pair, to produce states with a  $(\nu g_{9/2})^2 \otimes (\nu p_{1/2})^{-1}$  configuration. These states can occur at low energy due to the stronger coupling between nucleons in the  $g_{9/2}$  orbital. The isomeric state can then be understood to come from the  $J = 0$  coupling, while the  $3/2^-$  and  $5/2^-$  states could come from the  $J = 2$  coupling. However, this concept cannot explain the number of  $3/2^-$  and  $5/2^-$  states observed or their energy. In a weak coupling approach, the two states from the  $J = 2$  coupling should lie centered about the energy of the  $2_1^+$  in the adjacent even-even nuclei, which in this case is  $\sim 600$  keV.

It does not seem likely that strong deformation is involved (see, e.g., [5]) since either prolate or oblate deformation should result in a  $5/2^+$  ground state. The occurrence of a three-quasiparticle state seems the reasonable explanation since our data are consistent with a

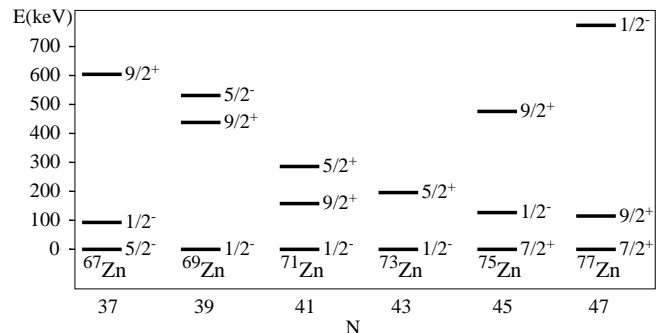


FIG. 12: Low-energy level systematics of odd-A  $Z=30$  zinc isotopes including the lowest  $1/2^-$  and  $9/2^+$  states in  $^{75}\text{Zn}$ . Energy levels in zinc are taken from [5], [12], [13], and the present work. For discussion, see text.

$7/2^+$  ground state and not  $9/2^+$ .

It is evident that a complex interplay of effects is involved in the structure of the heavy zinc isotopes. It is possible that large-basis shell-model calculations (see, e.g., [30]) could provide the answer. However, additional experimental work is needed to solidify the spin/parity assignments for all nuclei in this region.

## V. CONCLUSION

In the experiment on  $\beta$  decay of  $^{75}\text{Cu}$ , with a measured half-life of 1.222(8) s, the  $\gamma\gamma$  and  $\beta\gamma$  data were collected using the Low-energy Radioactive Ion Beam Spectroscopy Station. The data analysis revealed a previously unknown structure of  $^{75}\text{Zn}$  with some 120  $\gamma$ -ray transitions placed in a level scheme containing 59 levels including two states above the neutron separation energy. The latter finding may influence theoretical calculations of  $\beta$ -delayed neutron branching ratios in this nuclear mass range.

We have identified the  $1/2^-$  isomeric state at 127 keV in  $^{75}\text{Zn}$  which has remained elusive for a long time as well as a proposed  $9/2^+$  state at 476 keV. The transition of the ground state between the  $\pi p_{3/2}$  and the  $\pi f_{5/2}$  orbitals occurs between  $^{73}\text{Cu}$  and  $^{75}\text{Cu}$  [6] and, therefore, the detailed information on the decay of the transitional nucleus  $^{75}\text{Cu}$  is of particular importance. This information fills in the level systematics for the odd-A zinc isotopes and shows the relative similarity in their structures. However, additional experimental and theoretical

studies are needed to explain difference in the structures observed including the large number of additional states observed below 500 keV in  $^{75}\text{Zn}$ .

A more thorough study of the  $^{75}\text{Zn}$  low-energy level structure might be useful. In particular, a specifically designed conversion electron measurement would be needed to confirm our suggestion for a low-energy highly converted transition supposedly linking the 152- and 127-keV states. The present work also indicates that a closer look at the structure of  $^{73}\text{Zn}$  is needed.

## ACKNOWLEDGMENTS

We wish to acknowledge the Holifield Radioactive Ion Beam Facility (HRIBF) and staff for their help and the excellent quality of the neutron-rich beams. In addition, the engineering staff at the HRIBF, specifically Jim Johnson and Charles Reed, deserves our thanks for their help in constructing the Low-energy Radioactive Ion Beam Spectroscopy Station beam line. This research is sponsored by the Office of Science, U. S. Department of Energy under contract Grant Nos. DE-FG02-96ER41006, DE-FG02-96ER40983, DE-AC05-06OR23100, DE-FG02-96ER40978, and DE-FG05-88ER40407; National Nuclear Security Administration under the Stewardship Science Academic Alliances program through DOE Cooperative Agreement DE-FG52-08NA28552; Polish Ministry of Science and Higher Education Grant No. N N202 1033 33; and the Foundation for Polish Science.

- 
- [1] J. P. Schiffer, S. J. Freeman, J. A. Caggiano, C. Deibel, A. Heinz, C.-L. Jiang, R. Lewis, A. Parikh, P. D. Parker, K. E. Rehm, S. Sinha, and J. S. Thomas, *Phys. Rev. Lett.* **92**, 162501 (2004). [Issn: 0031-9007; Coden: PRLTAA] [DOI: 10.1103/PhysRevLett.92.162501]
- [2] L. Gaudefroy, O. Sorlin, D. Beaumel, Y. Blumenfeld, Z. Dombrádi, S. Fortier, S. Franchoo, M. Gélin, J. Gibelin, S. Grévy, F. Hammache, F. Ibrahim, K. W. Kemper, K.-L. Kratz, S. M. Lukyanov, C. Monrozeau, L. Nalpas, F. Nowacki, A. N. Ostrowski, T. Otsuka, Yu.-E. Penionzhkevich, J. Piekarewicz, E. C. Pollacco, P. Roussel-Chomaz, E. Rich, J. A. Scarpaci, M. G. St. Laurent, D. Sohler, M. Stanoiu, T. Suzuki, E. Tryggestad, and D. Verney, *Phys. Rev. Lett.* **97**, 092501 (2006). [Issn: 0031-9007; Coden: PRLTAA] [DOI: 10.1103/PhysRevLett.97.092501]
- [3] S. Michimasa, S. Shimoura, H. Iwasaki, A. Tamaki, S. Ota, N. Aoi, H. Baba, N. Iwasa, S. Kanno, S. Kubono, K. Kurita, A. Kurokawa, T. Minemura, T. Motobayashi, M. Notani, H. J. Ong, A. Saito, H. Sakurai, E. Takeshita, S. Takeuchi, Y. Yanagisawa, A. Yoshida, *Phys. Lett. B* **638**, 146 (2006). [DOI: 10.1016/j.nuclphysa.2006.12.086]
- [4] E. Runte, W.-D. Schmidt-Ott, P. Tidemand-Petersson, R. Kirchner, O. Klepper, W. Kurcewicz, E. Roeckl, N. Kaffrell, P. Peuser, K. Rykaczewski, M. Bernas, P. Dessagne, M. Langevin, *Nucl. Phys.* **A399**, 163 (1983). [DOI: 10.1016/0375-9474(83)90600-0]
- [5] M. Huhta, P. F. Mantica, D. W. Anthony, P. A. Lofy, J. I. Prisciandaro, R. M. Ronningen, M. Steiner, and W. B. Walters, *Phys. Rev. C* **58**, 3187 (1998). [Issn: 0556-2813; Coden: PRVCAN] [DOI: 10.1103/PhysRevC.58.3187]
- [6] K. T. Flanagan, P. Vingerhoets, M. Avgoulea, J. Billowes, M. L. Bissell, K. Blaum, B. Cheal, M. De Rydt, V. N. Fedosseev, D. H. Forest, Ch. Geppert, U. Köster, M. Kowalska, J. Krämer, K. L. Kratz, A. Krieger, E. Mané, B. A. Marsh, T. Materna, L. Mathieu, P. L. Molkanov, R. Neugart, G. Neyens, W. Nörtershäuser, M. D. Seliverstov, O. Serot, M. Schug, M. A. Sjoedin, J. R. Stone, N. J. Stone, H. H. Stroke, G. Tungate, D. T. Yordanov and Yu. M. Volkov, *Phys. Rev. Lett.* **103**, 142501 (2009). [Issn: 0031-9007; Coden: PRLTAA] [DOI: 10.1103/PhysRevLett.103.142501]
- [7] S. V. Ilyushkin, J. A. Winger, C. J. Gross, K. P. Rykaczewski, J. C. Batchelder, L. Cartegni, I. G. Darby, C. Goodin, R. Grzywacz, J. H. Hamilton, A. Korgul, W. Królas, S. N. Liddick, C. Mazzocchi, S. Padgett, A. Piechaczek, M. M. Rajabali, D. Shapira, and E. F. Zganjar, *Phys. Rev. C* **80**, 054304 (2009). [DOI: 10.1103/PhysRevC.80.054304]



- [8] N. Patronis, H. De Witte, M. Gorska, M. Huyse, K. Kruglov, D. Pauwels, K. Van de Vel, P. Van Duppen, J. Van Roosbroeck, J. -C. Thomas, S. Franchoo, J. Cederkall, V. N. Fedoseyev, H. Fynbo, U. Georg, O. Jonsson, U. Köster, T. Materna, L. Mathieu, O. Serot, L. Weissman, W. F. Mueller, V. I. Mishin and D. Fedorov, *Phys. Rev. C* **80**, 034307 (2009). [Issn: 0556-2813; Coden: PRV-CAN] [DOI: 10.1103/PhysRevC.80.034307]
- [9] T. Otsuka, T. Suzuki, R. Fujimoto, H. Grawe, and Y. Akaishi, *Phys. Rev. Lett.* **95**, 232502 (2005). [Issn: 0031-9007; Coden: PRLTAO] [DOI: 10.1103/PhysRevLett.95.232502]
- [10] K.-L. Kratz, H. Gabelmann, P. Müller, B. Pfeiffer, H. L. Ravn, A. Wüthrich, *Z. Phys. A* **340**, 419, (1991). [DOI: 10.1007/BF01290331]
- [11] P. L. Reeder, R. A. Warner, R. M. Liebsch, R. L. Gill, A. Piotrowski, *Phys. Rev. C* **31**, 1029 (1985). [DOI: 10.1103/PhysRevC.31.1029]
- [12] E. K. Lin, B. L. Cohen, *Phys. Rev.* **132**, 2632 (1963). [DOI: 10.1103/PhysRev.132.2632]
- [13] D. von Ehrenstein, J. P. Schiffer, *Phys. Rev.* **164**, 1374 (1967). [Issn: 0031-899X; Coden: PHRVAO] [DOI: 10.1103/PhysRev.164.1374]
- [14] E. Runte, K. L. Gippert, W.-D. Schmidt-Ott, P. Tidemand-Petersson, L. Ziegeler, R. Kirchner, O. Klepper, P. O. Larsson, E. Roeckl, D. Schardt, N. Kafrell, P. Peuser, M. Bernas, P. Dessagne, M. Langevin and K. Rykaczewski, *Nucl. Phys. A* **441**, 237 (1985). [DOI: 10.1016/0375-9474(85)90032-6]
- [15] National Nuclear Data Center, ENSDF database, <http://www.nndc.bnl.gov>.
- [16] S. B. Burson, W. C. Jordan and J. M. Le Blanc, *Phys. Rev.* **96**, 1555 (1954).
- [17] M. Goldhaber and A. W. Sanyar, *Phys. Rev.* **83**, 906 (1951).
- [18] B. Ekström, B. Fogelberg, P. Hoff, E. Lund, A. Sangariyavanish, *Phys. Scr.* **34**, 614 (1986). [Issn: 0031-8949; Coden: PHSTBO] [DOI: 10.1088/0031-8949/34/6A/017]
- [19] B. A. Tatum, *Nucl. Instr. and Meth. in Phys. Res.* **B241**, 926 (2005). [doi:10.1016/j.nimb.2005.07.171]
- [20] HRIBF's LeRIBSS website, <http://www.phy.ornl.gov/hribf/equipment/leribss/> (accessed August 2010).
- [21] R. Grzywacz, Experimental Equipment - Digital Pixies at HRIBF, <https://www.phy.ornl.gov/hribf/news/aug-10/ra3.shtml> (accessed November 2010).
- [22] J. A. Winger, S. V. Ilyushkin, K. P. Rykaczewski, C. J. Gross, J. C. Batchelder, C. Goodin, R. Grzywacz, J. H. Hamilton, A. Korgul, W. Królas, S. N. Liddick, C. Mazzocchi, S. Padgett, A. Piechaczek, M. M. Rajabali, D. Shapira, E. F. Zganjar, and I. N. Borzov, *Phys. Rev. Lett.* **102**, 142502 (2009). [Issn: 0031-9007; Coden: PRLTAO] [DOI: 10.1103/PhysRevLett.102.142502]
- [23] J. A. Winger, K. P. Rykaczewski, C. J. Gross, R. Grzywacz, J. C. Batchelder, C. Goodin, J. H. Hamilton, S. V. Ilyushkin, A. Korgul, W. Królas, S. N. Liddick, C. Mazzocchi, S. Padgett, A. Piechaczek, M. M. Rajabali, D. Shapira, E. F. Zganjar, and J. Dobaczewski, *Phys. Rev. C* **81**, 044303 (2010). [DOI: 10.1103/PhysRevC.81.044303]
- [24] S. Padgett, M. Madurga, R. Grzywacz, I. G. Darby, S. Paulauskas, M. Rajabali, C. J. Gross, K. Rykaczewski, D. Shapira, J. Winger, S. Ilyushkin, A. Korgul, W. Królas, S. N. Liddick, C. Mazzocchi, and E. Zganjar, *Phys. Rev. C*, in press.
- [25] S. Rahaman, J. Hakala, V.-V. Elomaa, T. Eronen, U. Hager, A. Jokinen, A. Kankainen, I. D. Moore, H. Penttil, S. Rinta-Antila, J. Rissanen, A. Saastamoinen, C. Weber and J. Äystö, *Eur. Phys. J. A* **34**, 2007. [DOI: 10.1140/epja/i2007-10489-y]
- [26] S. Baruah, G. Audi, K. Blaum, M. Dworschak, S. George, C. Guénaut, U. Hager, F. Herfurth, A. Herlert, A. Kellerbauer, H.-J. Kluge, D. Lunney, H. Schatz, L. Schweikhard, C. Yazidjian, *Phys. Rev. Lett.* **101**, 262501 (2008). [DOI: 10.1103/PhysRevLett.101.262501]
- [27] A. C. G. Mitchell and A. B. Smith, *Phys. Rev.* **85**, 152 (1952).
- [28] J. W. Mihelich, M. Goldhaber, and E. Wilson, *Phys. Rev.* **82**, 972 (1951).
- [29] J. A. Harvey, *Phys. Rev.* **81**, 353 (1951).
- [30] K. Sieja, F. Nowacki, *Phys. Rev. C* **81**, 061303 (2010). [DOI: 10.1103/PhysRevC.81.061303]